

Simultaneous moduli measurement of elastic materials at elevated temperatures using an ultrasonic waveguide method

Suresh Periyannan and Krishnan Balasubramaniam

Citation: *Review of Scientific Instruments* **86**, 114903 (2015); doi: 10.1063/1.4935556

View online: <http://dx.doi.org/10.1063/1.4935556>

View Table of Contents: <http://aip.scitation.org/toc/rsi/86/11>

Published by the *American Institute of Physics*



JANIS

**Janis Dilution Refrigerators & Helium-3 Cryostats
for Sub-Kelvin SPM**

Click here for more info www.janis.com/UHV-ULT-SPM.aspx

Simultaneous moduli measurement of elastic materials at elevated temperatures using an ultrasonic waveguide method

Suresh Periyannan and Krishnan Balasubramaniam^{a)}

Centre for Non Destructive Evaluation and Department of Mechanical Engineering,
Indian Institute of Technology Madras, Chennai 600 036, India

(Received 20 July 2015; accepted 25 October 2015; published online 20 November 2015)

A novel technique for simultaneously measuring the moduli of elastic isotropic material, as a function of temperature, using two ultrasonic guided wave modes that are co-generated using a single probe is presented here. This technique can be used for simultaneously measuring Young's modulus (E) and shear modulus (G) of different materials over a wide range of temperatures (35 °C–1200 °C). The specimens used in the experiments have special embodiments (for instance, a bend) at one end of the waveguide and an ultrasonic guided wave generator/detector (transducer) at the other end for obtaining reflected signals in a pulse-echo mode. The orientation of the transducer can be used for simultaneously generating/receiving the L(0,1) and/or T(0,1) using a single transducer in a waveguide on one end. The far end of the waveguides with the embodiment is kept inside a heating device such as a temperature-controlled furnace. The time of flight difference, as a function of uniform temperature distribution region (horizontal portion) of bend waveguides was measured and used to determine the material properties. Several materials were tested and the comparison between values reported in the literature and measured values were found to be in agreement, for both elastic moduli (E and G) measurements, as a function of temperature. This technique provides significant reduction in time and effort over conventional means of measurement of temperature dependence of elastic moduli. © 2015 AIP Publishing LLC. [<http://dx.doi.org/10.1063/1.4935556>]

I. INTRODUCTION

The dependence of Young's modulus (E) and shear modulus (G) of an elastic solid over a wide range of temperatures is required in the design and analysis of materials for engineering applications. This is particularly important when the material shall be used for elevated temperature applications such as in engines, power plants,^{1,2} or in order to understand its behaviour during a fire.³

Several methods have been reported in the literature for measurement of modulus vs temperature. The most common method, however elaborate and tedious, is to use individual tensile testing and shear testing approach inside a furnace. This method would involve several experiments, for each temperature, using extensive fixtures for loading the sample at these temperatures. An alternate approach would involve the use of ultrasonic waves and relate the measurement of wave velocities to the moduli (assuming that the density as a function of temperature is known *a priori*). In order to make such ultrasonic measurements, two approaches, i.e., (a) buffer rod waveguide approach,^{4–7} and (b) laser ultrasound approach,^{8–10} are well documented. While the Young's modulus may be measured using these approaches, the measurement of shear modulus is relatively more challenging.¹¹ Cook *et al.*,¹² developed a system for temperature dependent dynamic Young's modulus measurement of 4330 V steel using a longitudinal resonance method (the piezoelectric ultrasonic composite oscillator technique—PUCOT)

and compared it with a flexural resonance method (the impulse excitation technique—IET). Hill and Shimmin¹³ had determined the dynamic elastic moduli of 40 metals and alloys at room to elevated temperatures; the determinations were based on a relation between the speeds of sound in a material. Here, the specimen of the material was excited electrostatically and its resonant frequency determined, then the dynamic elastic modulus was calculated with respect to the geometry of the specimen. Farraro and McLellan,¹⁴ determined the Young's modulus and shear modulus of materials nickel, molybdenum, and platinum at a temperature range from 25 °C to 1000 °C using pulse echo waveguide approach. Lamidieu and Gault¹⁵ explained that ultrasonic longitudinal short pulses were generated by a magnetostrictive transducer in a ferro-magnetic rod, which was coupled to the sample via a refractory alumina waveguide, for investigating Young's modulus of the refractory concrete during heat treatment at working conditions of lining in a cement plant furnace. For different stainless steels (304, 310, and 316), the longitudinal and transverse velocities were measured using a pulse echo technique over a range of temperatures (4 K–295 K) and, then the elastic constants were calculated by Ledbetter.¹⁶ The Young's modulus vs temperature data was also tabulated for 40 metal alloys at a wide temperature range (0 K–590 K) by Ledbetter.¹⁷

The Young's modulus of aluminium tuning fork was measured by frequency variation data at different temperatures (29 °C–300 °C) by Greer,¹⁸ while Meena and Sahoo¹⁹ conducted the tensile test for aluminium specimen using universal testing machine at various ranges of temperatures (27 °C–325 °C) from which true stress and strain were calculated.

^{a)}Author to whom correspondence should be addressed. Electronic mail: balas@iitm.ac.in. Telephone: 044-22575688.

Jiyun²⁰ measured the physical properties of a solid material, such as the porosity ψ , pore shape-factor β , and elastic modulus E , by an ultrasonic sensor, which transmits and receives ultrasonic waves on the surface of the solid material.

Gault *et al.*²¹ used a magnetostrictive-based ultrasonic pulse echo technique for measurement of Young's modulus of the four large grained Al_2O_3 -based refractory materials up to 1800 °C. Here, a 200 kHz ultrasonic longitudinal pulse was transmitted and received through thin tungsten waveguide coupled to the sample (sample was a rectangular beam $2.5 \times 2.5 \times 70$ mm) via an Al_2O_3 waveguide at various temperatures. Huger *et al.*²² also used similar methods of measurement for Young's modulus of ceramic composite materials up to 1500 °C. Bichkov *et al.*²³ measured the Young's modulus of Zirconium-Niobium alloys up to 950 °C by measuring the natural frequency of vibration of a specimen in the form of cylindrical rod.

In this paper, a waveguide based approach for determining the two moduli (at the same time), using a single transducer that generates both longitudinal and torsional modes, as a function of temperature is described. Here, the material that is being examined is in the form of a waveguide (that is, a wire, rod, strip, etc.) and sufficiently long so that ultrasonic transduction (at different directions) can be accomplished on one end of the waveguide while the simultaneous (E and G) measurement is performed at the other end which is at controlled temperatures. The measurement end was kept inside a temperature-controlled furnace while the ultrasonic transducer was kept outside the furnace. In order to avoid the effects of the temperature gradients in the waveguide, an embodiment in the form of an L-bend was used at the end of the waveguide in order to obtain two reflections from the bend region. The relative time-of-flight of the individual wave modes $L(0,1)$, $T(0,1)$ can be related to the moduli of the waveguide $E(T)$ and $G(T)$, respectively, provided the temperature of the furnace is known. In order to measure $E(T)$ and $G(T)$, two incident wave modes were employed in a single experiment. In this work, the transducer coupled the ultrasonic waves into the waveguide using a very thin layer of viscous silicone based ultrasonic couplant.

Waveguide based sensors have been used for several measurement applications such as fluid level indication, flow front, density, temperature, and rheology measurement of the surrounding fluid. Lynnworth²⁴ summarized several waveguide sensors for *process control* applications. Balasubramaniam *et al.*,^{25,26} Prasad *et al.*,²⁷ and Pandey *et al.*,²⁸ measured time of flight (TOF) and amplitude (A) from the reflected ultrasonic signal from the end of a waveguide, which can be used for measuring the properties (product of density and viscosity) of molten material, in which the end was immersed. Visvanathan and Balasubramaniam²⁹ have also described the flow front monitoring inside molds using torsional waveguide.

Most of the previous works on ultrasonic waveguides have been used any one mode $L(0,1)$ or $T(0,1)$ to measure the physical properties of the surrounding fluid, where the elastic properties of the waveguide as a function of temperature were assumed to be known. In other works,^{4-7,15,21,23} elastic properties of materials were measured using ultrasonic wave $L(0,1)$ or $T(0,1)$ modes that were generated from an

ultrasonic transducer, that is located in ambient temperature, and transferred into a test sample that was located inside a hot zone. In our work, the elastic properties of the waveguide material are considered unknown while the physical properties of the surrounding fluid would be known *a priori*. In this paper, the surrounding fluid used was air and the influence of the variation of the bulk modulus of air with temperature, on the measurements made here, was assumed to be negligible.

In this work, the elastic moduli of different waveguide materials were simultaneously evaluated, using a single transducer (to generate and receive the $L(0,1)$, $T(0,1)$) that was excited using a single ultrasonic pulser-receiver unit. The waveguides were coupled to the transducer at different direction of orientations (0° or 45° or 90°) using a special transducer holder fixture. The local temperatures of a fluid around the bent portion of the waveguide (embodiment) influence the TOF for the round trip travel of $L(0,1)$ and $T(0,1)$ wave modes in the bent region. The time of flight difference $(\delta\text{TOF})_{L,T}$ was defined as the change in time of flight at measurement temperature compared to time of flight at room temperature in the horizontal bent region (uniform temperature distribution region) of the waveguide. The δTOF is due to two effects, that is, the change in the length of the waveguide due to coefficient of thermal expansion, and a change in the $L(0,1)$, $T(0,1)$ wave group velocity of material as a function of temperature. The $(\delta\text{TOF})_L$ data were used for measuring the material property $E_i(T)$ and $(\delta\text{TOF})_T$ was used for measuring $G_i(T)$. The $E_i(T)$ and $G_i(T)$ have been measured in the laboratory furnace over the range of 35 °C–1200 °C. It is also noted that the frequencies of generation of the guided wave modes $L(0,1)$ and $T(0,1)$ are selected so that they behave in a relatively non-dispersive manner.

Since multiple signals from the bend and the end of the waveguide have to be monitored during the heating and the cooling cycle, a multiple signal peak-tracking algorithm was employed to lock the time of flight measurement to specific signals of interest even though the signals are shifting in time during the heating process. Due to the rather long pulse-width and the relatively lower frequencies of the ultrasonic signals used to generate the guided wave modes, the maximum number of signals that must be simultaneously analyzed was found to be limited (time of flight measurements from each signal is limited due to signal overlap of closely spaced echoes). Here, the peak tracking algorithm uses several software "time gates" that are pre-set around the peaks of interest in the RF signals obtained from the waveguide. The number of "time gates" will depend on the number of peaks to be tracked. The time gate was 1.2 μs wide and the peak point was approximately located in the middle of the "time gates." In this current study, 4 "time gates" were employed for the two guided wave modes and for the two reflected signals of interests (one from the bend and one from the end). The time of flight of the peak value within the "time-gate" is recorded and archived. Subsequently during the heating and the cooling cycles, the location of these "time gates" was re-positioned (after each acquisition of the data and computation of the TOF) such that the peak stays located approximately in the middle of the "time gate" based on the previously measured TOF of the peak. Thus, the "time gate" will move with the signal and thereby ensuring that the TOF

measurements are performed even as the signals change with the temperature.

The $\delta\text{TOF}_{L,T}$ at different temperatures from a uniform temperature region (horizontal bent portion), for entire heating cycle, was then measured. Conventional shear wave transducer with a bandwidth of 0.25–0.5 MHz was used for simultaneously transmitting and receiving L(0,1) and T(0,1) modes, respectively.

II. DISPERSION ANALYSIS

The propagation of ultrasonic waves in waveguides has been well documented by Rose.³⁰ In a cylindrical waveguide, there are three families of modes, namely, longitudinal (L), torsional (T), and flexural (F), that can propagate along the axial direction (z) of a cylindrical rod with coordinates (r , θ , and z). Here, the analysis concentrates on the fundamental longitudinal L(0,1) and torsional T(0,1) modes. The mode has smaller levels of dispersion over a wide range of frequencies and can be easily generated in the rods made of high temperature materials.

The phase velocity dispersion curves were obtained using Disperse software developed by Pavlakovic *et al.*³¹ Phase velocity— V_p and group velocity— V_g dispersion curves (obtained from Disperse®) for rods of different diameters made of different high temperature materials are shown in Figures 1(a) and 1(b). The material properties and dimensions of the high temperature waveguides that are explored in this paper are shown in Table I. It can be noted that different materials have specific frequency ranges where the wave is non-dispersive as observed from Figures 1(a) and 1(b). It is desirable that,

TABLE I. Material properties and dimensions of waveguide materials.

Material	Mass density (ρ) (Kg m ⁻³)	Young's modulus (GPa)	Poisson's ratio (μ)	l, l_b, d (mm)
Kanthal	7250	215	0.30	740, 36, 1.58
Nickel	8950	218	0.31	900, 52, 1.50
Copper	9000	128	0.34	850, 51, 1.19
Aluminium	2710	71	0.33	1180, 51, 1.35
Platinum	21450	168	0.38	485, 51, 0.65

in the chosen frequency range, the waveguides must exhibit only a small degree of dispersion in order to keep the pulse width of the signals relatively narrow and hence to improve the reliability of TOF measurements. Hence, in order to maintain regions of low dispersion, appropriate diameters of the rods must be chosen.

III. METHODS OF ULTRASONIC TRANSDUCTIONS

A conventional ultrasonic normal x-cut PZT based shear wave transducer (Panametrics/Olympus NDT V151) is placed on one side of a nickel wire waveguide such that the plane of the surface of the transducer is tangential to the circumference of the waveguide. Since the shear wave has a fixed polarisation of vibration, three directions of orientations between the transducer and waveguide axis (0°, 45°, and 90°) were used to generate different modes as listed by the 3 case studies as discussed below and elaborated in the Figures 2-4. For these experiments, the bend waveguide (nickel) dimensions

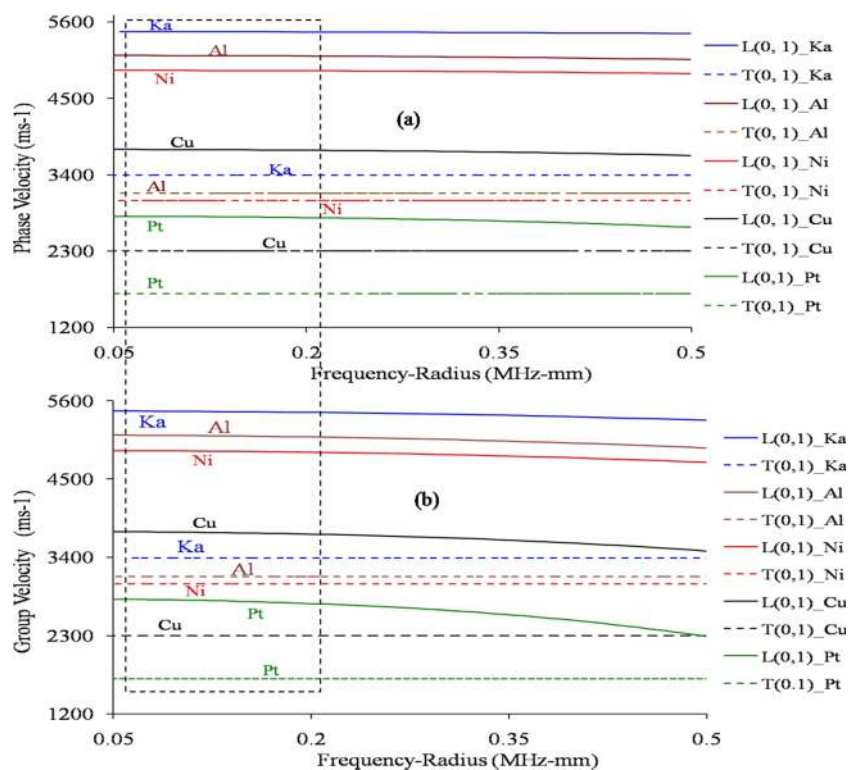


FIG. 1. (a) and (b) Dispersion curves (phase velocity— V_p and group velocity— V_g) for L(0,1), T(0,1) modes for different materials and dimensions of materials as per Table I.

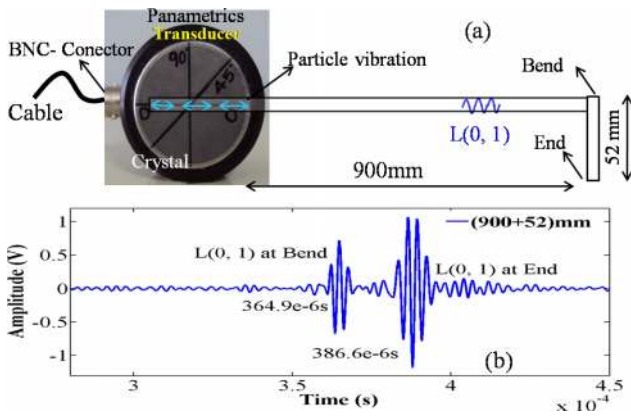


FIG. 2. (a) Shear wave transducer orientation is parallel (0°) to the axis of waveguide, (b) the reflected L(0,1) signals are obtained from the bend (900 mm) and end (952 mm) of a waveguide.

are followed by Table I and appropriate excitation frequency range was chosen from Figures 1(a) and 1(b).

A. Case 1

When the angle is 0° , i.e., the vibration is along the axis of the waveguide, L(0,1) wave mode is generated and received. The experimental setup is shown in Figure 2(a) and the A-scan of the RF signal obtained using this pulse-echo transmit-receive approach is shown in Figure 2(b). The L(0,1) wave mode reflected signals from the bend region and the end of the waveguide is clearly observed. Hence, the first reflected (at $364.9 \mu s$) signal is from the bend in waveguide and the second signal is the reflection (at $386.6 \mu s$) from the end of waveguide. The difference in the time of flights (i.e. $21.7 \mu s$) between two signals was used for measuring the E(T). Other mode converted signals are also present, but due to the relatively slower velocities of these modes, these could be avoided by time-gating the first two signals representing the pure L(0,1) mode reflections from the bend and the end. Also, the mode converted signals are polarized at an angle that is not aligned with the preferred orientation of the probe, thereby providing only weaker signals that can be ignored.

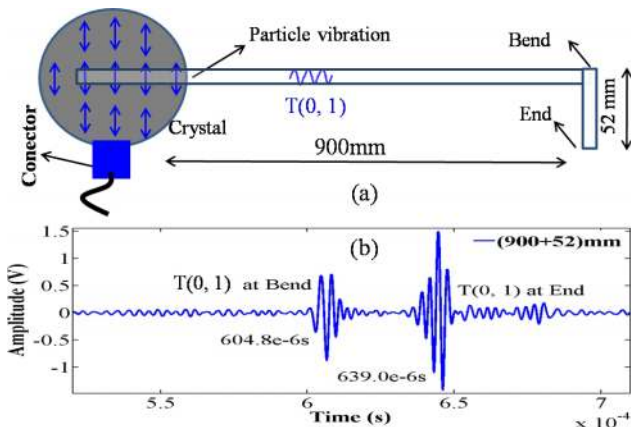


FIG. 3. (a) Shear wave transducer orientation is perpendicular (90°) to the axis of waveguide, (b) the reflected T(0,1) signals are obtained from the bend (900 mm) and end (952 mm) of a waveguide.

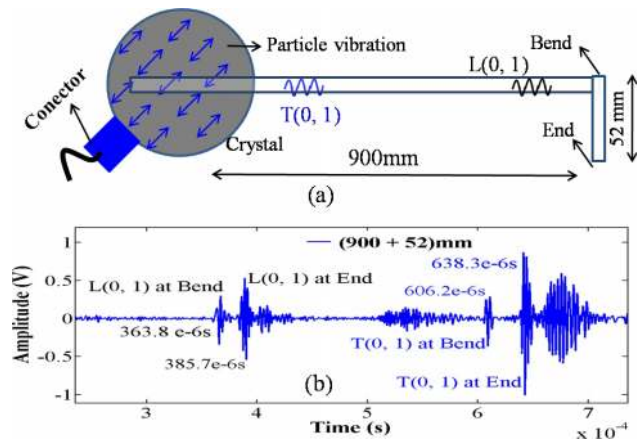


FIG. 4. (a) Shear wave transducer orientation is 45° to the axis of the waveguide, (b) the reflected L(0,1) and T(0,1) mode signals are obtained simultaneously from the bend (900 mm) and end (952 mm) of a waveguide.

B. Case 2

When the angle is 90° , i.e., the vibration is perpendicular to the axis of the waveguide, T(0,1) wave mode is generated and received as shown in Figure 3(a). Again the T(0,1) modes are clearly identified from the bend region and the end as observed from the Figure 3(b). Here, again the T(0,1) modes are clearly identified since the mode converted signals are not efficiently detected by the polarized transducer. The A-scan in Figure 3(b) shows the first reflected signal (at $604.8 \mu s$) from the bend of the waveguide and the second reflected signal (at $639 \mu s$) from the end of the waveguide. It must be observed that, as expected, the time of flight of the signals are approximately twice that of the L(0,1) modes represented in Figure 2(a).

C. Case 3

When the angle is 45° , i.e., the vibration is along the axis of the waveguide, both L(0,1) and T(0,1) wave modes are simultaneously generated and received as shown in Figure 4(a). Again, it is clear from the A-scan signals that the 4 individual signals from the reflections from the two wave modes from the bend and the end are clearly identified as shown in Figure 4(b). However, there are mode converted signals that are of smaller amplitude but clearly noticeable. However, the appropriate signals can be identified from the time of flight measurements that were previously determined in Figures 2(b) and 3(b). It is the focus of this paper to demonstrate the simultaneous generation and reception of both wave modes and to utilize this for the measurement of the temperature dependent moduli E(T) and G(T) using a single experiment. It is necessary to take the dispersion curve and the group velocity of the two wave modes in order to select the bend-length, the frequency, and the dimensions (diameter and length) of the waveguide in order to minimize the mode conversion effects. However, in our experiments, it was found that this for a wide range of materials, the signals obtained were of similar nature and the four individual signals were clearly recognized. Once the signals were identified, a peak tracking algorithm³² was used during the experiment to lock the reference points on each of

these signals and follow the change in the time of flight of these reference points during the heating cycles of the measurement.

IV. EXPERIMENTAL SETUP

Figure 5(a) illustrates the transducer holder and actual schematic view of the experimental setup used and Figure 5(b) shows the bent waveguide dimensions as well as the transducer holder. The transducer is securely held by the fixture, then the wave guide can be connected with transducer at different orientations (0° , 45° , and 90°) using different slots from the holder fixture.

A. Experimental procedure and measurement

In order to avoid the effects of temperature gradients on the long straight portion of the waveguide, the bent region of the waveguide is kept horizontal so that there is minimal temperature gradient (if any) across the bent region in Figure 5(a). Hence, the measurements of E and G are related to the material property in the bent region of material at the ambient temperature. Also co-located with the waveguide bend region, a K-type thermocouple was placed for simultaneous measurement of temperature. The thermocouple data were recorded in a PC using the National Instruments USB based NI 9211 card for temperature read out. A Panametrics (Olympus NDT) 5077 Pulser/Receiver was coupled to the transducer and used to transmit/receive the ultrasound through waveguides. The Olympus (Panametrics) model 5077PR provided a negative square wave excitation with a fast pulse rise and fall time (<20 ns each). The pulse voltage (100–400 V) and pulse width were adjusted directly to provide precise control over pulse shape by tuning to the desired frequency bandwidth (0.25–0.5 MHz). A National Instruments USB NI5133 A/D convertor (100 MHz, 8 bit) was used to interface the ultrasonic pulser/receiver to the PC for data acquisition and archival of the digital signals. A peak-tracking algorithm based on an earlier reported algorithm Periyannan and Balasubramaniam³² was implemented in the software for the dynamic signal peak following the 4 signals during the heating of the waveguide. The dynamic signal peak following algorithm ensured that the

TOF measurements were extremely reliable and repeatable. An insulated resistive heating (6 kW) furnace was used for the steady state heating of the waveguide that employed a Shinko programmable controller. In this furnace, maximum temperature was achieved 1450°C .

Three case studies are used, at different positions of same waveguide and along with shear wave transducer orientations for this work. In the first case, a transducer was employed for axial excitation (0°) to generate L(0,1) mode on the waveguide to measure the Young's modulus (E) of material. In the second case, transducer was employed for tangential excitation (90°) to generate T(0,1) mode on the waveguide to measure the shear modulus (G) of material. For the last case, the same transducer was employed (45°) for the simultaneous excitations L(0,1) and T(0,1) to measure E and G of material, thus allowing measurement of material's E and G using a single set of experiment.

B. Temperature dependent E and G measurement relations using ultrasonic guided waves

The bent region of the waveguide that is located in the uniform temperature distribution region of the furnace was used for the evaluation of $(\text{TOF}_0)_{L,T}$ and $(\delta\text{TOF}_i)_{L,T}$ using Equations (1) and (2) at various temperatures. Here, the temperature variations have been assumed to be only in the vertical direction. Any temperature gradient in the horizontal direction within the bent region has been neglected. E and G at a given temperature “i” due to a change in L(0,1) and T(0,1) mode's δTOF at horizontal portion of the waveguide (due to temperature variations) in Figures 3–5 can be calculated using the arguments and expressions provided as follows:

$$(\text{TOF}_0)_{L,T} = [(\text{TOF}_b - \text{TOF}_a)]_{L,T} \quad \text{at the room temperature } (T_0), \quad (1)$$

$$(\delta\text{TOF}_i)_{L,T} = [(\text{TOF}_{bi} - \text{TOF}_{ai}) - (\text{TOF}_b - \text{TOF}_a)]_{L,T}. \quad (2)$$

From Eqs. (1) and (2),

$$(\text{TOF}_i)_{L,T} = (\text{TOF}_0)_{L,T} + (\delta\text{TOF}_i)_{L,T} \quad \text{at the instantaneous temperature } (T_i), \quad (3)$$

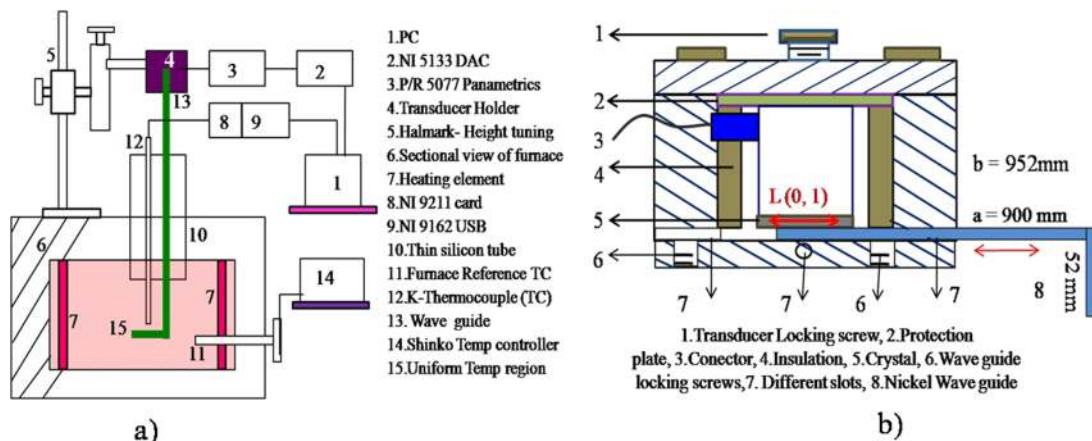


FIG. 5. (a) Schematic diagram of the experimental setup with waveguide bend-region inside a furnace and (b) waveguide along with the sectional view of the flexible transducer holder.

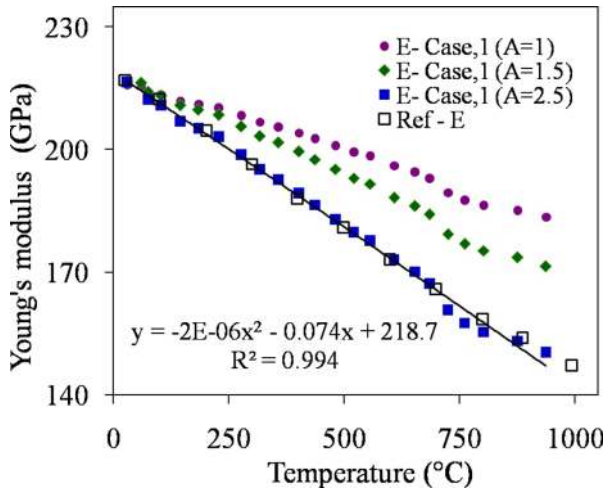


FIG. 6. Temperature vs experimental E_i for different trials and different values of A for nickel waveguide and comparison with the literature data for nickel E_i ³⁵ in order to evaluate the empirical constant A .

where

- subscripts L and T are related to $L(0,1)$ or $T(0,1)$ wave modes in the bent waveguides;
- subscripts a and b are related to the dimensions of bent waveguide.

The waveguide material normal (E) and shear moduli (G) were calculated at various temperatures based on $(\delta TOF)_{L,T}$ and TOF measurements using the empirical relationships obtained for the computation of instantaneous elastic moduli (E_i and G_i) at any given temperature for a given E_0 , G_0 and by measurement of δTOF 's using $L(0,1)$ wave mode for E_i and $T(0,1)$ mode for G_i , respectively, as in Equations (4) and (5) explained in more detail elsewhere by Periyannan and Balasubramaniam,³³

$$E_i = \left(\frac{E_0}{1 + A \left(\frac{\delta TOF_i}{TOF_0} \right)_L} \right), \quad (4)$$

$$G_i = \left(\frac{G_0}{1 + B \left(\frac{\delta TOF_i}{TOF_0} \right)_T} \right). \quad (5)$$

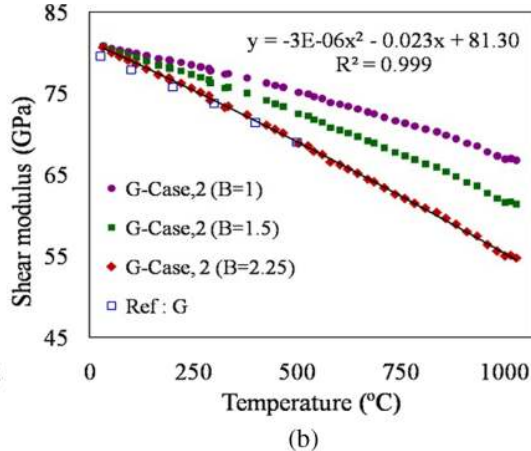
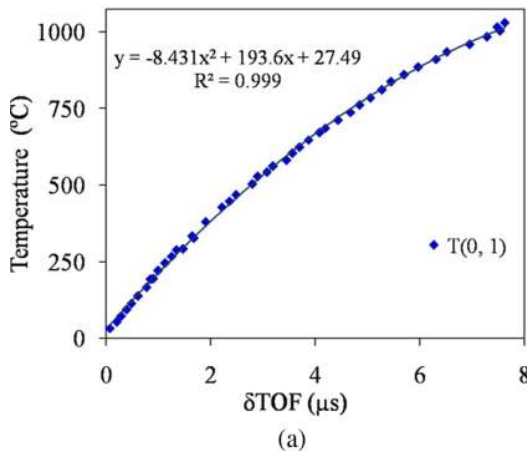


FIG. 7. (a) and (b) The δTOF_T vs temperature and G_i of the waveguide (nickel³⁶) at various temperatures, respectively, and comparison with the literature data in order to obtain the best fit value for B .

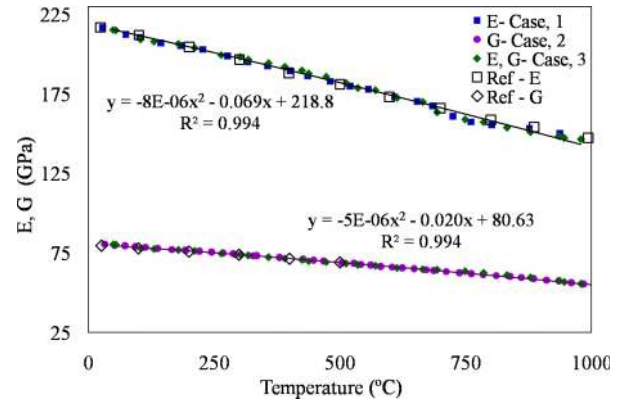


FIG. 8. Temperature vs experimental E_i , and G_i , with verification using data from Refs. 35 and 36 for nickel.

In these empirical equations, the constants A and B were found to be constants and material independent. Some of the preliminary results on this approach have been reported elsewhere.^{33,34} However, a more detailed set of experiments were conducted as described below.

V. ESTIMATION OF EMPIRICAL CONSTANTS (A AND B) FOR E, G MEASUREMENTS OF MATERIAL

A. Case 1: Young's modulus measurement using $L(0,1)$ mode of a nickel waveguide

A waveguide, made from nickel, with dimensions as described in Figures 2(a) and 2(b) was used in the experiment with the bent horizontal region inside a temperature controlled furnace. The waveguide attached to an ultrasonic transducer that generates $L(0,1)$ mode was initially considered in the experiment. The direction of transducer excitation was oriented parallel to the axis of the waveguide. The $(\delta TOF_i)_L$ values were measured using Equation (2) at instantaneous temperatures that were measured by placing a calibrated K-type thermocouple positioned near the horizontal bent portion of the waveguide. The measurements were obtained during the heating cycle.

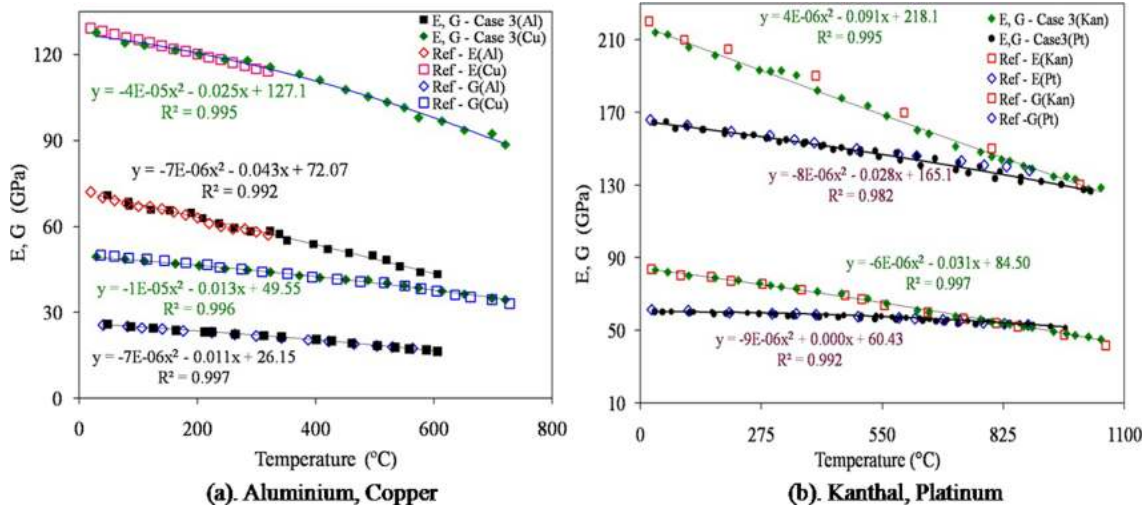


FIG. 9. (a) and (b) Temperature vs Experimental E_i and G_i of four different materials, verified with the literature data.

The E_i values computed using Equation (4) at various temperatures for different values of constant A, are shown in Figure 6. Using the best fit approach, the constant A was measured to be 2.50. Similarly, experiments were conducted using T(0,1) mode and the empirical constant value was extrapolated to other materials and evaluated found to work well for all of the different metals tested.

B. Case 2: Shear modulus measurement using T(0,1) of a nickel waveguide

In order to generate the torsional mode, a shear wave transducer was used to produce tangential excitation with an orientation perpendicular to the waveguide axis as shown in Figure 3(a) and the experimental setup used was similar to Figure 5(a). All experiments were carried out using 0.5 MHz frequency and the previous experimental procedure was followed. The $(TOF_0)_T$ and $(\delta TOF_i)_T$ for the T(0,1) mode were measured, for heating cycle using Equations (1) and (2), and the results are shown for nickel waveguide in Figure 7(a). The G_i values obtained were found to compare well with the published material in the literature.³⁶ In Figure 7(b) and using previously described empirical equation (Equation (5)), the empirical constant B was determined to be equal to 2.25 for computing G_i from the measured TOF for the T(0,1) mode. Again, this empirical constant was found to be valid for a wide range of materials and will be used henceforth in this paper.

C. Case 3: Simultaneous E and G measurements of nickel material

In the last case, shear wave transducer was orientated (45° inclination) to the surface axis of waveguide. Here, the simultaneously excited L(0,1) and T(0,1) modes were generated. The bend reflected and the mode-converted signals from these two modes were also received by the same transducer, in a pulse-echo mode, as shown in Figure 3(a). The time of flights of both modes are noted in the same figure and also the velocities were verified with individual measurements from cases 1 and 2. Similar procedures and equations were used for simultaneous E_i and G_i measurements of nickel material using case 3 setup. Hence, case 3 allows the measurement of E_i and G_i of the material using a single setup of experiment. Finally, the measured instantaneous E_i and G_i values (from case 3) of nickel material were validated with the literature as well as compared to cases 1 and 2 are shown in Figure 8. The fine agreement can be observed between the case studies and the literature data in the same figure. The similar approach (case 3) can be adopted for different materials.

VI. ELASTIC MODULI MEASUREMENTS OF COPPER (Cu), ALUMINIUM (Al), KANTHAL, AND PLATINUM (Pt)

Similar to the above description, the E_i and G_i measurements of 4 different materials Kanthal, Pt, Cu, and Al at various temperatures were conducted. The dimensions of different

TABLE II. Second order polynomial fit coefficients for $E_i(T)$ (left) and $G_i(T)$ (right) of the materials evaluated.

Material	$E_i(T) = aT_1^2 + bT_1 + c$				$G_i(T) = dT_1^2 + eT_1 + f$			
	A	b	c	R^2	d	e	f	R^2
Nickel	-8.00×10^{-06}	-0.069	218.8	0.994	-5.00×10^{-06}	-0.020	80.63	0.994
Kanthal	4.00×10^{-06}	-0.091	218.2	0.995	-6.00×10^{-06}	-0.031	84.50	0.997
Platinum	-8.00×10^{-06}	-0.028	165.1	0.984	-9.00×10^{-06}	0.000	60.43	0.992
Copper	-4.00×10^{-05}	-0.025	127.1	0.995	-1.00×10^{-05}	-0.013	49.55	0.996
Aluminium	-7.00×10^{-06}	-0.043	72.07	0.992	-7.00×10^{-06}	-0.011	26.15	0.997

TABLE III. Percentage of error from E_i measurements of materials at various temperatures.

Temperature (°C)	Kanthal	Platinum	Nickel	Copper	Aluminium
30	1.06	0.80	0.72	1.66	0.24
100	1.67	0.61	0.33	0.64	0.12
200	2.40	0.43	0.21	0.36	0.44
400	3.31	0.46	0.57	0.45	0.62
600	3.32	1.02	0.26	...	1.65
800	2.07	2.20	1.00
1000	1.00	4.08	3.49

materials (L-bent waveguides) are shown in Table I and the experimental frequency range was chosen from Figures 1(a) and 1(b). Subsequently, experimental E_i and G_i values of different materials were verified with the different literature data,^{1,17,35,37–39} as shown in Figures 9(a) and 9(b).

A. Analysis of E_i and G_i measurement

Table II shows the second order polynomial fit coefficients for $E_i(T)$ and $G_i(T)$ of different materials along with the correlation coefficient R^2 as measured using the ultrasonic waveguide method. The polynomial expressions for temperature dependent behaviour of E_i and G_i are provided below in Equations (6) and (7), respectively,

$$E_i(T) = \mathbf{a}T_i^2 + \mathbf{b}T_i + \mathbf{c}, \quad (6)$$

$$G_i(T) = \mathbf{d}T_i^2 + \mathbf{e}T_i + \mathbf{f}. \quad (7)$$

The high correlation in the curve fit parameters and the excellent matching between the experimentally obtained values along with the published data demonstrate that this method can be reliably and efficiently used to obtain temperature dependent moduli values for a variety of elastic materials.

B. Comparison of the obtained results with literature data

The error analysis was done (using Equation (8)) for different materials for the simultaneous measurements of E_i and G_i from ultrasonic waveguide approach with the literature values at different temperatures, as shown in Tables III and IV.

TABLE IV. Percentage of error from G_i measurements of materials at various temperatures.

Temperature (°C)	Kanthal	Platinum	Nickel	Copper	Aluminium
30	0.53	1.35	0.71	1.34	0.48
100	0.42	1.84	0.65	1.03	1.14
200	0.43	0.61	0.54	0.55	1.90
400	0.48	1.84	0.21	0.52	2.59
600	1.17	1.42	0.30	1.87	1.68
800	2.68	1.73	1.00
1000	3.88	1.81	1.98

Here,

$$\% \text{ Error} = \frac{|\text{Literature value} - \text{Experimental value}|}{\text{Literature value}} \times 100. \quad (8)$$

VII. CONCLUSION

A novel ultrasonic waveguide technique is reported, which uses a bent waveguide to simultaneously measure the elastic moduli (E_i and G_i) of different materials over a wide range of temperatures. Three case studies, using a transducer at different direction of orientations (0° or 45° or 90°), for generating/receiving independently as well as simultaneously the $L(0,1)$ and/or $T(0,1)$ wave modes. All three cases of the time of flight differences $(\delta\text{TOF})_{L,T}$ were measured at the horizontal bent portion (uniform temperature region) of waveguide. The $(\delta\text{TOF})_{L,T}$ could then be used to calculate $E_i(T)$ and $G_i(T)$ of the waveguide material as a function of temperature using two empirical constants based expressions. The empirical constants A and B were determined experimentally. Simultaneous mode measurements for the moduli $E_i(T)$ and $G_i(T)$ were compared well with independent mode measurements and were also validated with data found in the literature. The simultaneous technique can be used for rapid and efficient measurement of temperature dependent elastic moduli of materials over a wide range of temperatures. This technique has the potential to provide a time saving and robust alternative to other existing techniques for measurement of high temperature moduli properties.

ACKNOWLEDGMENTS

The authors wish to thank the Board for Research in Nuclear Sciences (BRNS), Mumbai, INDIA, for financial support for this work.

- ¹R. B. McLellan and T. Ishikawa, *J. Phys. Chem. Solids* **48**, 603 (1987).
- ²E. Ufuah, "Characterization of elevated temperature mechanical properties of butt-welded connections made with HS steel grade S420M 2012," in *Proceedings of the World Congress on Engineering (WCE, London, UK, 2012)*, Vol. III.
- ³J. Outinen, O. Kaitila, and P. Makelainen, "A study for the development of the design of steel structures in fire conditions," in 1st International Workshop of Structures in Fire, Copenhagen, Denmark, 2000.
- ⁴S. M. Kumaran, V. Rajendran, T. Jayakumar, P. Palanichamy, P. Shankar, and B. Raj, *J. Alloys Compd.* **464**, 150 (2008).
- ⁵L. Bourgeois, M. H. Nadal, F. Clement, and G. R. Chapuis, *J. Alloys Compd.* **444–445**, 261 (2007).
- ⁶A. Sather, *J. Acoust. Soc. Am.* **43**, 1291 (1968).
- ⁷E. Schreiber, O. L. Anderson, and N. Soga, *Elastic Constants and Their Measurement* (McGraw-Hill, New York, 1973).
- ⁸M. H. Nadal, C. Hubert, and G. R. Chapuis, *J. Alloys Compd.* **444–445**, 265 (2007).
- ⁹R. S. Lima, S. E. Kruger, G. Lamouche, and B. R. Marple, *J. Therm. Spray Technol.* **14**, 52 (2005).
- ¹⁰J. A. Brammer and C. M. Percival, *Exp. Mech.* **10**, 245 (1970).
- ¹¹Y. Bao, H. Zhang, M. Ahmadi, M. A. Karim, and H. F. Wu, *Ultrasonics* **54**, 867 (2014).
- ¹²L. S. Cook, A. Wolfenden, and G. M. Ludtka, *Dynamic Elastic Modulus Measurements in Materials* (ASTM, STP, 1990), Vol. 1045, pp. 81–95.
- ¹³W. H. Hill and K. D. Shimmin, "Elevated temperature dynamic elastic moduli of various metallic materials," Wadd Technical Report 60, 438, 1961.
- ¹⁴F. Farraro and R. B. McLellan, *Meteorol. Trans. A* **8**, 1553 (1977).

- ¹⁵P. Lamidieu and C. Gault, *Mater. Sci. Eng.* **77**, 11 (1986).
- ¹⁶H. M. Ledbetter, *J. Appl. Phys.* **52**, 1587 (1981).
- ¹⁷H. M. Ledbetter, *Cryogenics* **22**, 653 (1982).
- ¹⁸Z. L. Greer, *ISB J. Phys.* **5**, 1 (2011).
- ¹⁹A. Meena and S. K. Sahoo, Tensile Test of Aluminium at High Temperatures Report, NIT, Rourkela, India, 2010.
- ²⁰T. Jiyun, "Method for measuring physical properties of solid material," Agency Industrial Science Technology patent JPH 08189923 (10 January 1995).
- ²¹C. Gault, F. Platon, and D. Le Bras, *Mater. Sci. Eng.* **74**, 105 (1985).
- ²²M. Huger, D. Fargeot, and C. Gault, "High-temperature measurement of ultrasonic wave velocity in refractory materials," *High Temperatures - High Pressures* **34**(2), 193–201 (2002).
- ²³Y. F. Bichkov, A. N. Rozanov, and D. M. Skorov, *J. Nucl. Energy* **5**, 408 (1957).
- ²⁴L. C. Lynnworth, *Ultrasonic Measurements for Process Control: Theory, Techniques, Applications* (Academic Press, New York, 1989).
- ²⁵K. Balasubramaniam, V. V. Shah, D. Costley, G. Bourdeaux, and J. P. Singh, *Rev. Sci. Instrum.* **70**, 1 (1999).
- ²⁶K. Balasubramaniam, V. V. Shah, D. Costley, G. Bourdeaux, and J. P. Singh, U.S. patent 6,296,385 (2 October 2001).
- ²⁷V. S. K. Prasad, K. Balasubramaniam, E. Kannan, and K. L. Geisinger, *J. Mater. Process. Technol.* **207**, 315 (2008).
- ²⁸J. C. Pandey, M. Raj, S. N. Lenka, S. Periyannan, and K. Balasubramaniam, *J. Iron Making Steel Making* **38**, 74 (2011).
- ²⁹K. Visvanathan and K. Balasubramaniam, *Rev. Sci. Instrum.* **78**, 015110 (2007).
- ³⁰J. L. Rose, *Ultrasonic Waves in Solid Media* (Cambridge University Press, 1999), pp. 143–152.
- ³¹B. N. Pavlakovic, M. J. S. Lowe, P. Cawley, and D. N. Alleyne, *Rev. Prog. Quant. Nondestr. Eval.* **16**, 185 (1997).
- ³²S. Periyannan and K. Balasubramaniam, *Measurement* **61**, 185 (2015).
- ³³S. Periyannan and K. Balasubramaniam, "Temperature dependent E and G measurement of materials using ultrasonic guided waves," *AIP Conf. Proc.* **1581**, 256 (2014).
- ³⁴K. Balasubramaniam and S. Periyannan, "A novel waveguide technique for the simultaneous measurement of temperatures dependent properties of materials," World Intellectual Property Organization patent WO 2015/008299 A2 (22 January 2015).
- ³⁵R. Farrao and R. B. McLellan, *Metall. Trans. A* **8**, 1563 (1977).
- ³⁶Special Metals Corporation, publications are Nickel 200 and Nickel 201, 1–2 (2014), available online at www.specialmetals.com.
- ³⁷Kanthal-D Datasheet updated 20 June 2012, available online at www.kanthal.com.
- ³⁸M. H. Nadal and P. LePoac, *J. Appl. Phys.* **93**, 2472 (2003).
- ³⁹W. C. Overton and J. Gaffney, *Phys. Rev.* **98**, 969 (1955).